PHILOSOPHICAL TRANSACTIONS A

rsta.royalsocietypublishing.org

Research

Article submitted to journal

Subject Areas:

xxxxx, xxxxx, xxxx

Keywords:

xxxx, xxxx, xxxx

Author for correspondence:

B. Ganapathisubramani

e-mail:

g.bharath@southampton.ac.uk

Modelling high Reynolds number wall-turbulence interactions in laboratory experiments using large-scale free-stream turbulence

Eda Dogan, R. Jason Hearst and Bharathram Ganapathisubramani

Engineering and the Environment, University of Southampton, Southampton, United Kingdom, SO17 1BJ

A turbulent boundary layer subjected to free-stream turbulence is investigated in order to ascertain the scale interactions that dominate the near-wall region. The results are discussed in relation to a canonical high Reynolds number turbulent boundary layer because previous studies have reported considerable similarities between these two flows. Measurements were acquired simultaneously from four hot-wires mounted to a rake which was traversed through the boundary layer. Particular focus is given to two main features of both canonical high Reynolds number boundary layers and boundary layers subjected to free-stream turbulence: (i) the footprint of the large scales in the logarithmic region on the near-wall small scales, specifically the modulating interaction between these scales, and (ii) the phase difference in amplitude modulation. The potential for a turbulent boundary layer subjected to free-stream turbulence to "simulate" high Reynolds number wall-turbulence interactions is discussed. The results of this study have encouraging implications for future investigations of the fundamental scale interactions that take place in high Reynolds number flows as it demonstrates that these can be achieved at typical laboratory scales.

THE ROYAL SOCIETY PUBLISHING

1. Introduction

As the Reynolds number of a turbulent boundary layer grows, the energy signature of the large scales encroaches on that of the near-wall turbulence [1]. In boundary layers, the large energetic motions in the outer region, known as superstructures, carry a significant portion of the turbulent kinetic energy, contributing to a significant amount of the Reynolds stresses in these flows [2–4]. These superstructures become more energetic and exhibit a footprint of increasing significance in the near-wall region with increasing von Kármán number ($Re_\tau = U_\tau \delta/\nu$) [5]. Hutchins and Marusic [1] showed that this footprint can extend deep into the near-wall region and lead to an increase in the near-wall streamwise turbulence intensities (in inner-scaling). They also showed that these large scales in the outer region tend to modulate the amplitude of the small-scale fluctuations in the near-wall region [6]. This sort of interaction between the scales has been examined before by Bandyopadhyay and Hussain [7] for various shear flows, including boundary layers, mixing layers, wakes and jets. They found significant coupling between these scales across all shear flows by correlating the low-frequency component (i.e., low-pass filtered time-series data from their hot-wire measurements) with a signal similar to the envelope of the high-frequency component. Mathis et al. [8] expanded on the findings of Hutchins and Marusic [6] and quantified the modulation across the boundary layer as the correlation coefficient, R, between the large-scale streamwise fluctuating velocity and an envelope of the small-scale fluctuations. Their profiles of R provided supporting evidence of amplitude modulation of the near-wall small scales by the large scales. They also noted that the modulating effect of the large scales increases with increasing Reynolds number. While there are certainly many open questions relating to how these scale interactions take place in high Reynolds number flows, there are also numerous limitations of performing measurements in the near-wall region of said flows, e.g., sensor spatial and temporal resolution, wall proximity errors [9,10]. Therefore, there is high demand for accurately predicting the near-wall turbulence with only large-scale information input [10,11].

In an attempt to isolate the influence of the large scales, Jacobi and McKeon [12–14] and Duvvuri and McKeon [15] introduced a single synthetic large scale into the boundary layer. Specifically, Duvvuri and McKeon [15] found that exciting the turbulent boundary layer by a large-scale input modifies the phase relationships naturally existing between the large and small scales of the turbulent boundary layer. These phase relationships were quantified in their study by the skewness of the streamwise velocity fluctuations and the amplitude modulation coefficient as previously suggested in the literature [16,17]. As opposed to a single dominant large-scale input, Dogan et al. [18] introduced a broadband set of large-scales centred about 10δ into their boundary layer with tailored free-stream turbulence (FST). They generated the FST using an active grid at the inlet of the wind tunnel test-section. They observed that the characteristics of their turbulent boundary layer in the presence of FST and canonical high Reynolds number turbulent boundary layers were similar with respect to the scale interactions. This is particularly significant because the presence of FST generated higher Re_τ in their facility than achievable under canonical conditions. This implies that the introduction of FST above the boundary layer can be used to simulate the near-wall interactions of a high Reynolds number turbulent boundary layer without the need of a specialised (very large) boundary layer facility. In their study, Dogan et al. [18] showed that the large scales have a modulating effect on the small scales in the near wall region and that this effect becomes more significant with increasing FST. The increasing FST results in more energetic large scales that simulate the increase in large-scale energy observed in high Reynolds number flow facilities for increasing Reynolds number, Re_τ. This similarity has encouraging implications for generalising scale interactions in turbulent boundary layers and mimicking high Reynolds number wall-flows in laboratory scale facilities. The current study builds on that of Dogan et al. [18] by replicating the FST and boundary layer conditions and performing measurements with multiple hot-wires simultaneously. The focus of this work is thus understanding the modulating interaction and phase relationships between the inner and outer

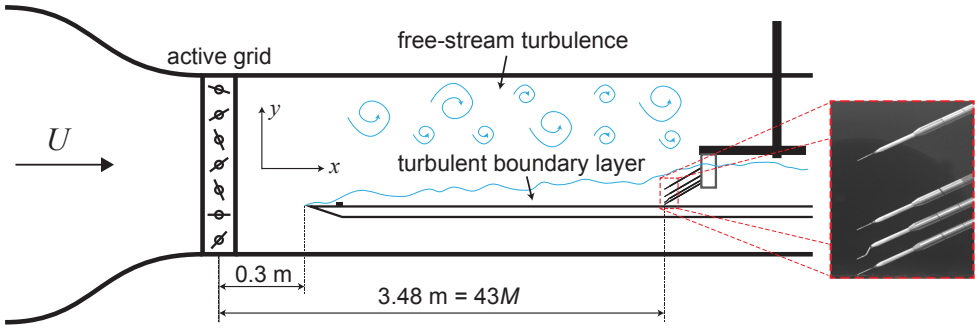

Figure 1: Schematic of the experimental set-up.

scales. Implications relating to the potential of modelling high Reynolds number wall-turbulence interactions in laboratory experiments using large-scale FST will be discussed.

2. Experimental procedure

The experimental design used here is a deliberate duplication of the study of Dogan et al. [18], except that we acquire data from four wires simultaneously. Full details on the facility and design can be found in [18]. In summary, the suction-type wind tunnel has a 0.9 m $\times$ 0.6 m $\times$ 4.5 m test-section and the boundary layer was formed on a suspended floor. Free-stream turbulence was generated with an active grid. A schematic of the experimental design is provided in figure 1.

Data were acquired from four hot-wires simultaneously. The wires were mounted to a rake with the probes angled into the boundary layer at 30^{o}. The second, third, and fourth wires were separated from the first by 7, 22, and 55 mm, respectively. This rake was then traversed using an automated stepper system over the range $0.4 \text{ mm} \leq y \leq 223$ mm. All wires were made in-house from tungsten wire mounted to Dantec-style prongs and had a nominal sensing length of 1 mm. The second wire in the rake was a boundary layer probe in order to position it in close proximity to the first wire. All other wires were standard single-wire probes. The wires were operated by a Dantec 54N82 multi-channel constant temperature anemometer at an overheat of 1.8. The wires were calibrated *in situ* with 15 points fitted to a fourth-order polynomial. Data were acquired at 20.5 kHz for a minimum of 6 minutes, which is ample time to converge the relevant statistics [18]. An analog filter was set at 10 kHz, and in post-processing the data were filtered with a fifth-order digital Butterworth filter at 7.5 kHz as it was observed that there was no meaningful signal beyond this frequency. The data were acquired with a National Instruments (NI) PXIe-1062Q 16-bit system. In particular, a NI TB-2709 card was employed because it allowed for simultaneous acquisition of multiple signals with dedicated A/D converters without the need of a multiplexer, thus ensuring no phase offset between signals.

This study replicates cases B and D from [18]; we maintain this naming convention for consistency. These two cases are both at $Re_x = 2.2 \times 10^6$ (with x = 0 at the leading-edge of the suspended flat plate). Relevant parameters from the present study are provided in table 1, and were calculated in the same manner as described in [18]. All gradient quantities were estimated using a sixth-order centred-differencing scheme as recommended in [19]. The flow characteristics

Table 1: (Colour online) Free-stream and turbulent boundary layer parameters for the study cases evaluated at the measurement location, $x/M = 43$.

FST cases	$U_\infty\ (m/s)$	$u'_\infty/U_\infty\ (\%)$	$Re_{\lambda,\infty}$	$\delta\ (m)$	$U_\tau\ (m/s)$	Re_τ	Re_θ
B (◆)	9.9	8.1	465	0.13	0.42	3590	4500
D (■)	10.1	12.2	630	0.16	0.43	4550	5340

provided in table 1 agree with those presented in [18] for the same cases to within the uncertainty margins. Furthermore, our mean profiles collapse well with the old data. Thus, the measurements are repeatable, and our multi-wire rake and the angle of the probes do not significantly influence the flow or measurements.

3. Amplitude modulation: Single-point measurements

Figure 2 shows spectrograms, mean profiles and variance profiles for both case B and D. The details of the figure are given in the figure caption. The prominent feature of both spectrograms is the presence of an outer peak similar to high Reynolds number flows [6]. This outer peak is within the logarithmic region of the boundary layer as seen in the mean profile. The outer peak is located close to the knee of the variance profile, where the variance starts to decrease above this wall-normal location. These features are consistent with existing data on canonical high Reynolds number turbulent boundary layers.

It can be seen that the energy of the outer peak grows with increasing turbulence intensity due to the increasing energy content of the large-scales in the free-stream. These high-energy scales in the free-stream penetrate the boundary layer and attain a local maximum within the outer region of the boundary layer. In this sense, the increase in FST can be viewed as "simulating" an increase in Re_τ for a canonical boundary layer. It should also be noted that the peak in the premultiplied energy spectrum occurs at length scales near 10δ, which is consistent with the energetic scales of high Reynolds number turbulent boundary layers. This dominant scale was in fact a deliberate choice made when establishing the scales of the FST. It is certainly possible to change this dominant scale by altering the active-grid operation mode as well as by altering the location of the flat plate relative to the grid. In this study, we are specifically interested in isolating the scale interactions where the energy containing large-scales are of $\mathcal{O}(10\delta)$ and therefore, we chose the mode of grid operation to produce these dominant scales.

The energetic scales in the free-stream (as well as the outer region) have a footprint in the near-wall region. There is a shift of the energy towards long wavelengths (i.e., low wavenumbers) very near the wall. The extent of the penetration depends on the FST level and this essentially "simulates" the effect of increasing Reynolds number. Correspondingly, the amplitude of the near-wall peak in the variance profiles is amplified with increasing FST level. In addition to this direct effect reaching down to the wall, the large-scales in the boundary layer under the influence of FST have been observed to modulate the amplitude of the small-scales in the near-wall region [18].

Dogan et al. [18] examined the above-mentioned interaction using the scale-decomposed skewness analysis of the streamwise velocity fluctuations as previously performed in [15,20,21]. The flow was decomposed into large and small scales using a sharp spectral cut-off filter [6,8] at a wavelength of $\zeta_x^+ \approx 4000$. The amplitude modulation coefficient is [8]:

$$R = \frac{\overline{u_L^+ \, E_L(u_S^+)}}{\sigma_{u_L^+} \, \sigma_{E_L(u_S^+)}} \tag{3.1}$$

where u_L^+ is the large-scale fluctuations, $E_L(u_S^+)$ is the filtered envelope of the small-scale fluctuations, $\cdot^+$ indicates inner scaling, and σ is the standard deviation. This coefficient is employed to quantify the level of modulation across the boundary layer as assessed by a single-wire using the same cut-off filter (the horizontal dashed line in plots (i) of figure 2) to separate the scales as large and small as the component of the energy above or below the cut-off, respectively. For both cases, the level of correlation is high in the viscous layer of the boundary layer suggesting a high level of modulation of small scales in the near-wall region. This correlation decreases until a plateau is reached and then in the logarithmic region it reaches its minimum value.

The location of the minimum correlation is observed to coincide with the outer spectral peak. For high Reynolds number canonical boundary layers, the correlation coefficient reaches zero at the outer spectral peak location above which the correlation is reversed [6,8]. Here, the reversal

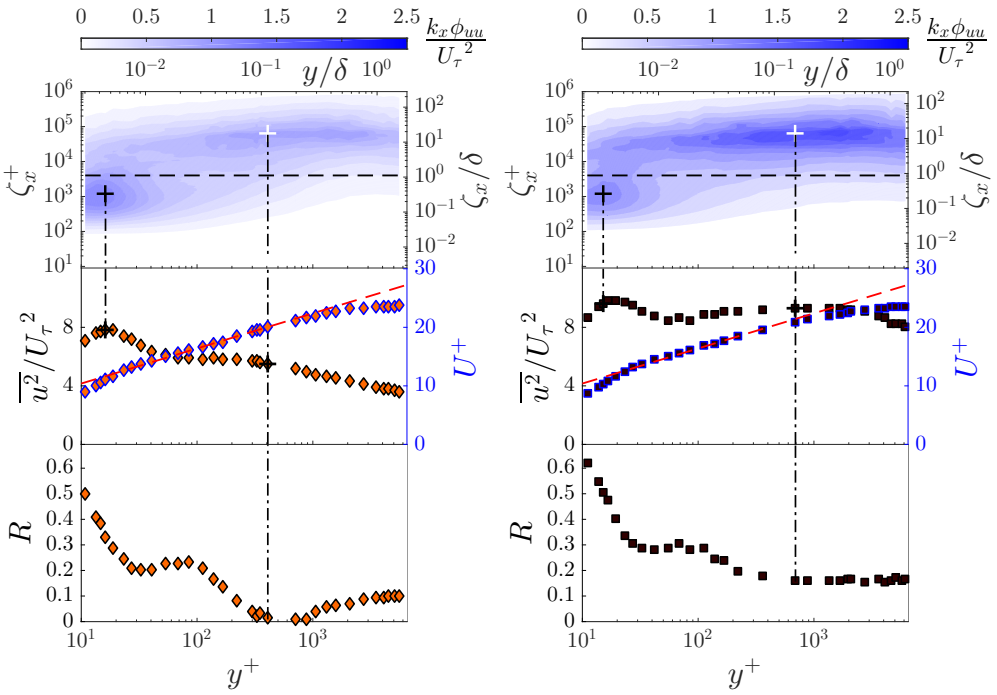

Figure 2: (i) Contour maps of the inner-normalised pre-multiplied energy spectra of the streamwise velocity fluctuations, $k_x\phi_{uu}/U_\tau^2$, for (◆) case B (left) and (■) case D (right). The ordinates show streamwise wavelength, ζ_x, in both inner (left) and outer (right) scaling. The abscissas show the wall-normal location, y, also plotted in both inner (bottom) and outer (top) scaling. (+) indicates inner (black) and outer (white) spectral peaks. The horizontal dashed line represents the location of the cut-off wavelength at $\zeta_x^+ \approx 4000$. (ii) Corresponding mean (blue outlined marker) and variance profiles. Dashed red line: log-law with coefficients $\kappa = 0.384$ and $A = 4.4$. Dot-dashed vertical lines and (+) symbols represent the locations corresponding to the spectral peaks indicated on (i). (iii) Amplitude modulation coefficient, $R\left(y^+\right)$, as defined in equation 3.1. Dot-dashed vertical lines follow the corresponding outer spectral peaks.

in correlation behaviour is not observed in the presence of FST. The lack of reversal is primarily related to a reduction in the intermittency in the outer part of the boundary layer when FST is present. The small-scale fluctuations in a canonical boundary layer have a distinct relationship to the large scales as they rely on these large scales for their energy and organisation. However, the small scales in the outer region of the current study are also influenced by the small scales of the FST. These FST-based small scales may not have any relationships to the large scales within the boundary layer and therefore mask the correlation reversal that might exist if it were possible to only consider the small scales that are relevant to the boundary layer. Nonetheless, the similarity between the scale interactions in the near-wall region of the present flow and high Reynolds number boundary layers is remarkable.

The local minimum in the buffer region is higher for the higher FST case. The increasing trend in the local minimum correlation value, as also observed by [18] for more FST cases is similar to the Reynolds number dependence of the modulation coefficient for a canonical boundary layer [21], i.e., increasing FST is akin to increasing Re_τ of a canonical boundary layer. Therefore, a turbulent boundary layer under the effect of FST can be seen as one way of emulating the scale

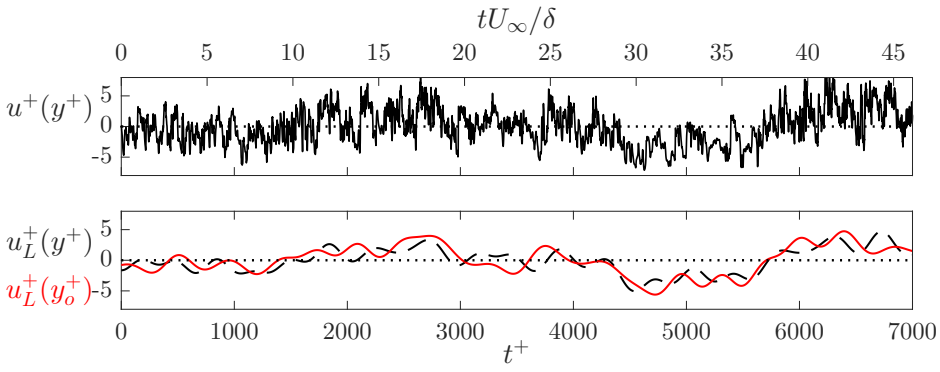

Figure 3: A sample of the inner-scaled fluctuating streamwise velocity signal for case B. (Top) raw fluctuating signal, $u^+(y^+)$, at $y^+ \approx 20$; (bottom) dashed line: large-scale fluctuating signal, $u_L^+(y^+)$, at $y^+ \approx 20$, solid line: large-scale fluctuating signal, $u_L^+(y_o^+)$, at $y_o^+ \approx 210$.

interactions that happen in the near-wall region of high Reynolds number turbulent boundary layers.

4. Amplitude modulation: Multi-point measurements

Although single-point measurements were found to provide a reasonable estimate of the degree of amplitude modulation, multi-point synchronised measurements are preferred for the study of interactions between the outer-region and the near-wall region because several assumptions of the former analysis can be relaxed in place of direct observations. As such, the analysis that follows employs the first two wires in the rake described in section 2.

A sample of the fluctuating streamwise velocity signal in inner-scaling from the inner probe and the large-scale fluctuations from both probes are given in figure 3 for case B. The inner probe is at $y^+ \approx 20$ around the near-wall peak and the outer probe is at $y_o^+ \approx 210$ in the log-region where the energy of the large scales is dominant. A high degree of correlation is visible from the large-scale fluctuations at the two different wall-normal locations. This correlation is found to be $\sim 80\%$. This is higher than 65% found in [11] for a canonical turbulent boundary layer that was justified as a result of the footprint caused by the superstructure-type events in the log region. The fact that the correlation is higher in FST cases supports the direct penetration of the FST large scales into the boundary layer and down to the near-wall region (this correlation is even higher for case D, $\sim 85\%$).

Given the similarities of the scale interactions with that of high Reynolds number canonical boundary layers, there is grounds to test the predictive inner-outer model of Marusic et al. [10], also detailed in Mathis et al. [11], for the turbulent boundary layers in the presence of FST. This would confirm the analogy between the two flows and validate the applicability of the model to this non-canonical case. Their model is able to predict the near-wall turbulence using only the large-scale information input. With this input, the predicted velocity signal at a wall-normal location is linked to a universal signal (a signal that is free from any large-scale influence) through the model coefficients. Figure 6 shows a schematic for the mathematical formulation of the predictive model. It should be noted here that the outer probe shifted large-scale signal in the formulation for FST cases, $u_{oL}^+(y_o^+, \theta_L)$, is different compared to a canonical case because for FST cases the large-scale signal also includes the FST large-scales that penetrate into the boundary layer. It is also worth mentioning that the two probes in the present study are both moving whereas only the inner probe moved with the outer probe fixed in [11]. However, here, the inner probe moves significantly in wall units whereas the outer probe can be said to be relatively fixed

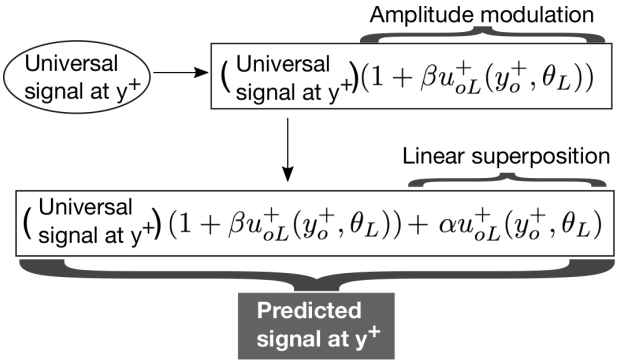

Figure 4: Mathematical formulation of the predictive inner-outer model of Marusic et al. [10] as given in [11]. y^+: inner probe location; β: model coefficient for amplitude modulation; $u^+_{oL}(y^+_o, \theta_L)$: filtered outer probe signal shifted forward in the streamwise direction for the corresponding θ_L where θ_L is the mean inclination angle of the large-scale structures; y^+_o: outer probe location; α: model coefficient for linear superposition.

relative to the main features of the flow. Therefore, this difference in the probe configuration is not expected to affect the results.

Briefly, the predictive model incorporates four different things: (i) a universal signal that would exist in the absence of any large-scale influences (ii) the inclination of the large-scale structures with the wall, θ_L, which will lead to a time-delay in the interaction, (iii) the superposition of the large-scale fluctuation on the near-wall region, represented by model coefficient α, and (iv) amplitude modulation of the small scales by the superimposed large scales, represented by model coefficient β. The details of the model and the procedure to calculate these coefficients can be found in [11].

The three aforementioned parameters of the predictive model are given for different wall-normal positions in figure 5 in comparison with the values from Mathis et al. [11]. The superposition coefficient is related to the correlation between the large-scale fluctuations of the two probes, the relation of which has already been demonstrated in figure 3 instantaneously at one specific wall-normal location. Here, when we look at the evolution of the coefficient in the wall-normal direction for all locations below the outer spectral peak, we can easily see a high degree of correlation throughout. This correlation is higher for case D (higher turbulence intensity) compared to case B (lower turbulence intensity). This confirms the observation from the spectrograms that the energy levels that reside in the near-wall region due to the penetration of FST increase with turbulence level in the free-stream. When compared with α values from [11] for a canonical case, higher values are observed for FST cases. This is a result of FST scales penetrating the boundary layer. The model takes into account the inclination angle of the large-scale structures; therefore requires shifting the outer probe signal forward in the streamwise direction (assuming Taylor's hypothesis) for the corresponding time shift between the large-scale signals from both probes. The inclination angle is typically within 12° and 16°, c.f., [11] and references therein including [22–24]. The present study exhibits similar large-scale structural organisation with an inclination angle that is relatively constant between $11^\circ < \theta_L < 15^\circ$ for wall-normal locations $y^+ < 150$. Although FST disturbs the boundary layer from outside, the fact that it does not destroy the large-scale structural organisation in the log-region is a promising result for establishing the analogy with high Reynolds number canonical flows. Beyond that wall-normal location where the two probes get closer in wall-units (in physical units the probes are a set distance apart), the angle is found to increase and reach around 20° as justified by the presence of increasingly correlated small-scale structures that have higher inclination angles [11].

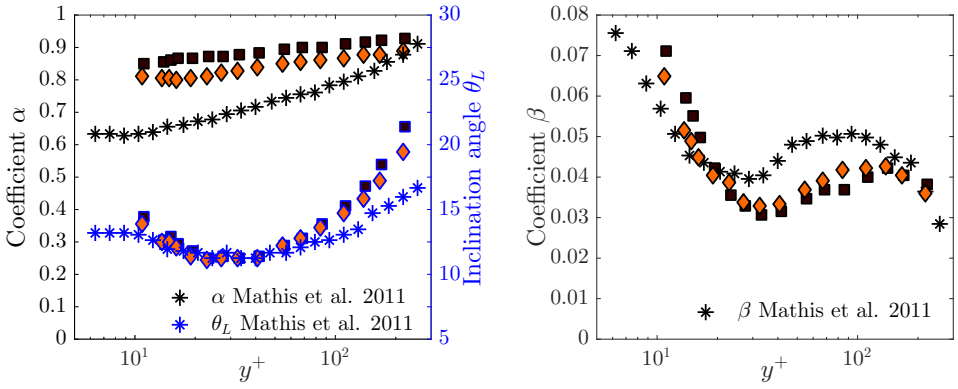

Figure 5: Wall-normal evolution of the predictive inner-outer model coefficients in comparison with Mathis et al. [11]. (Left) the superposition coefficient α and the mean inclination angle of the large-scale structures, θ_L (the blue outlined markers); (right) the amplitude modulation coefficient, β. (◆) case B, (■) case D, and (∗) Mathis et al. [11].

The value of β, which captures the modulation effect of the large scales on the envelope of the small scales in the turbulent boundary layer, gives similar results to the canonical case studied in [11] especially in the near-wall region. Nonetheless, the trend in β is observed to be similar to the trend in R (figure 2(iii)), which was also true for the canonical case of [11]. Since R indicates how much the signal is amplitude-modulated, β would be expected to indicate a similar trend to de-amplitude modulate this signal in order to remove the large-scale influence as similarly justified in [11]. This similarity also confirms that amplitude modulation of the scale interactions in the near-wall region is reasonably well represented in this "simulated" high Reynolds number flow. The magnitude of this coefficient is found to be smaller compared to the canonical case in [11]. When this model was applied to non-canonical cases like turbulent boundary layers subjected to pressure gradients in [25], the β values were similarly observed to be smaller compared to the canonical case in [11]. Agostini and Leschziner [26] claimed that although this predictive model correctly represents the superposition effects of the large scales through the superposition coefficient α, it does not capture entirely the asymmetry in the modulation with β coefficient. If we interpret our β results based on their observations, these asymmetries could be said to be stronger for a non-canonical flow and therefore additional factors might come into play when calculating β.

Finally, the universal signal can be determined using these model parameters. Since this signal is "universal" and thus independent of any large-scale influence, the signal for the two FST cases would not be expected to differ significantly. This is also verified through the variance distribution of the two signals determined as the universal signals for the two FST cases (not shown here for brevity). Once these model parameters are established, we could predict the signal in the near-wall region by using only large-scale signal input from a nominal peak in the outer region. Figure 6 presents the predicted and the measured values for the variance of the near-wall peak. Here, the aim is to validate the above model for various FST cases in addition to the two particular cases from the present study. As such, figure 6 is composed of data from Dogan et al. [18], which includes the present two cases and several others (see the original source for details on all cases). The predicted values are corrected for spatial resolution using the method of Chin *et al.* [27]. The prediction seems to work quite well for the FST cases with 75% R-squared value calculated for the identity line. The discrepancies from the equality line can be mainly due to (i) the difference in spectral filtering used for the scale separation and (ii) the limited wall-normal position range

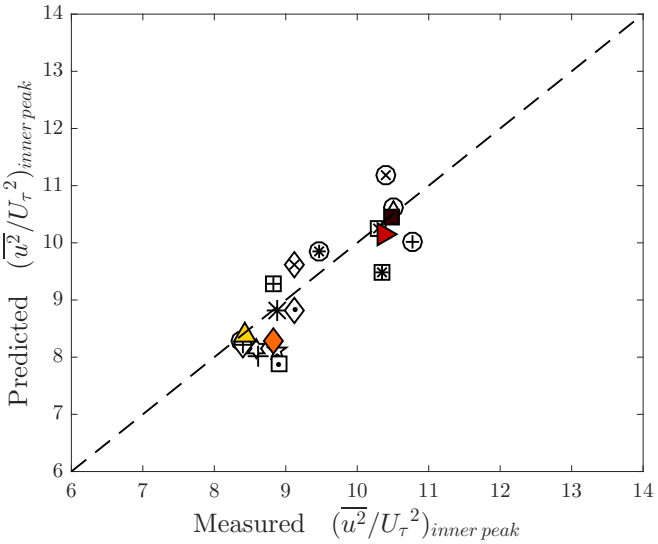

Figure 6: Predicted vs measured values of the inner-normalised near-wall peak variance of the streamwise velocity fluctuations. Details for all FST cases can be found in [18].

of the calibration experiment (i.e. the present experiment to calculate the model coefficients) that could pose an inefficiency of the method for the cases where the spectral outer peak location is out of the calibrated range. Regardless, the validity of the model suggests that this approach could be generalised to capture the influence of "any" large-scale influence on near-wall turbulence.

5. Phase information: Single point measurements

A phase difference between the large and small scales was found for amplitude modulation in previous studies and it was observed to increase with increasing distance from the wall [7,16,17]. Since the amplitude modulation coefficient is a correlation coefficient between the large scales and the envelope of the small scales, it could help define the phase relationship between them. However, Jacobi and McKeon [14] noted the nature of the phase relationship was obscured when examined with the correlation coefficient since the correlation is computed at zero time-lag while a phase difference necessarily means a non-zero time-lag. Therefore, they suggested employing the cross-correlation function itself. Following their suggestion, the time shift (or the phase difference), relationship across the whole boundary layer is investigated in figure 7 with cross-correlation contour maps from single point measurements. The phase difference is positive across the whole boundary layer implying that the envelope of the small-scale fluctuations leads the large-scale fluctuations in the boundary layer, in agreement with previous work [14,16,17]. This phase difference is found to increase with wall-normal position, also in agreement with previous studies [7,14,16,17,28]. However, unlike previous studies, the phase reversal is not observed for FST cases. This might be related to the increased small-scale fluctuations in the outer region of the boundary layer resulting from the FST. Nonetheless, the inner region phase relations are similar to a canonical boundary layer, which is promising as it indicates that the present methodology can be used to approximate the phase organisation of the large scales and the envelope of the small scales in high Reynolds number flows.

Duvvuri and McKeon [15] showed that the phase relations naturally existing in the flow between the scales can be modified by introducing a synthetic large scale. They suggested that the envelope of all small scales can be in-phase or out-of-phase with the synthetic large scale depending on its location with respect to the location of the critical layer (this is the layer where

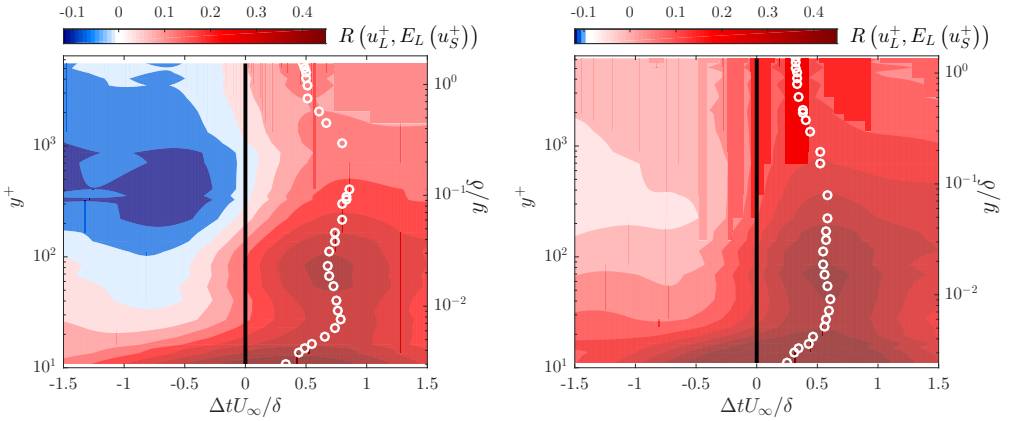

Figure 7: Contour maps of the cross-correlation between the large scales and the filtered envelope of the small-scales, $R(u_L^+, E_L(u_S^+))$. White circle markers depict the maximum correlation points. (Left) case B; (right) case D. The ordinates show the wall normal location, y, plotted in both inner (left) and outer (right) scaling. The abscissas show the time domain in outer scaling.

the wave speed of the disturbance is equal to the local mean velocity). They interpreted the zero-crossing location of their amplitude modulation coefficient as an indication of phase reversal, which in turn could point to the presence of the critical layer. The present amplitude modulation coefficient plots (figure 2) do not cross zero. This suggests that the critical layer tends to move towards the free-stream for higher intensity disturbances (and/or disturbances that are over a range of scales). This also implies that for broadband, high intensity forcing in the free-stream, it might not be possible to match the wave speed of a given disturbance to the mean velocity within the boundary layer and therefore the small- and large-scales remain in-phase. It must be noted that the wave speed of the disturbances in these FST cases is not known. However, if we assume Taylor's hypothesis for FST, the energetic motions that are injected by the active grid in the free-stream would be expected to advect at the mean velocity of the free-stream. If this is the case, then, it would not be possible for the local mean within the boundary layer to match the "wave speed" of the external disturbance. It is also plausible that a penetrated FST disturbance might travel within the boundary layer at a "wave speed" between the local mean and the free-stream velocity. In this case, one would expect to find a critical layer inside the boundary layer. However, since the disturbances have a broadband spectrum, the critical layer of each disturbance would be expected to be weak and therefore would result in a smeared collection of critical layers across which the phase can change only gradually. Since both explanations could lead to lack of phase reversal, further extensive work on phase relationships in the presence of broadband forcing is needed for any firmer conclusions.

6. Conclusions

This study has expanded on that of Dogan et al. [18] by complementing their work with simultaneous multiple-wire measurements in a turbulent boundary layer subjected to FST. The focus was on the similarities of the present flow with canonical high Reynolds number turbulent boundary layers. Adding FST results in more energetic large scales that simulate the increase in large-scale energy observed in high Reynolds number flow facilities for increasing Reynolds number, Re_τ. The potential to "simulate" high Reynolds number flows without requiring very large boundary layer facilities has been explored in detail by comparing the two flows specifically in terms of interactions and phase organisation between the scales.

The FST imposes a spectral peak in the outer region that resembles the naturally occurring spectral peak in canonical high Reynolds number boundary layers. These large scales were observed to modulate the amplitude of the near-wall small scales. This modulation was quantified by a modulation coefficient as previously done in the literature [8]. The scale interactions observed in the boundary layer subjected to FST resembled those of a high Reynolds number boundary layer. The predictive inner-outer model of Marusic et al. [10] was implemented for the present cases in order to test the analogy between these flows. The analogy was confirmed by comparing the present model coefficients to those of high Reynolds number flows. Since the aim of the model is to be able to predict the near-wall turbulence with only large-scale input, this analogy implies there is some universality, even under extreme free-stream conditions, of the large-scale influence on the near-wall turbulence.

It was also found that the envelope of the small-scale fluctuations led the large-scale fluctuations in the boundary layer as previously found for a canonical boundary layer [14,16,17]. The inner region phase relations of a canonical boundary layer were well captured here indicating the ability of the FST cases to maintain the phase organisations observed in canonical high Reynolds number flows.

The near-wall turbulence has significant relevance in an engineering context since drag-reducing control strategies are usually based on manipulating the near-wall structures [5]. Any factors that influence these structures, including the footprint of the large-scale structures in the log-region of the boundary layer as we explored here, should be taken into consideration for effective control strategies. Therefore, the potential to model high Reynolds number near-wall turbulence in laboratory scales using FST has encouraging implications towards developing robust flow control techniques needed for these high Reynolds number flows.

Data Accessibility. Supporting data for the figures present in this paper are accessible via: (*DOI to be included in future drafts*).

Authors' Contributions. ED and RJH carried out the experiments. ED performed the analysis and led the writing of sections 1 and 3-6. RJH wrote section 2. The study was conceived and designed in meetings attended by all three authors and spearheaded by BG. All authors read, contributed to the writing of, and approved the manuscript.

Competing Interests. The authors declare that they have no competing interests

Funding. The authors acknowledge the financial support of the European Research Council (ERC Grant agreement No. 277472), and the Engineering and Physical Sciences Research Council of the United Kingdom (EPSRC Grant Ref. No. EP/I037717/1). ED acknowledges the financial support of Zonta International. RJH acknowledges the financial support of the Natural Sciences and Engineering Research Council of Canada (NSERC).

Acknowledgements. The authors are grateful to Dr. R. Bleischwitz for his aid in designing and building the active grid, and the anonymous referees for their input.

References

1. Hutchins N N, Marusic I. 2007 Evidence of very long meandering features in the logarithmic region of turbulent boundary layers.
Journal of Fluid Mechanics **579**, 1–28.
2. Ganapathisubramani B, Longmire EK, Marusic I. 2003 Characteristics of vortex packets in turbulent boundary layers.
Journal of Fluid Mechanics **478**, 35–46.
3. Guala M, Hommema SE, Adrian RJ. 2006 Large-scale and very-large-scale motions in turbulent pipe flow.
Journal of Fluid Mechanics **554**, 521–542.
4. Balakumar B, Adrian R. 2007 Large- and very-large-scale motions in channel and boundary-layer flows.
Philosophical Transactions of the Royal Society of London A: Mathematical, Physical and Engineering Sciences **365**, 665–681.

5. Smits AJ, McKeon BJ, Marusic I. 2011 High-reynolds number wall turbulence.
Annual Review of Fluid Mechanics **43**, 353–375.
6. Hutchins N, Marusic I. 2007 Large-scale influences in near-wall turbulence.
Philosophical Transactions of the Royal Society A: Mathematical, Physical and Engineering Sciences **365**, 647–664.
7. Bandyopadhyay PR, Hussain AKMF. 1984 The coupling between scales in shear flows.
Physics of Fluids **27**, 2221–2228.
8. Mathis R, Hutchins N, Marusic I. 2009 Large-scale amplitude modulation of the small-scale structures in turbulent boundary layers.
Journal of Fluid Mechanics **628**, 311–337.
9. Hutchins N, Nickels TB, Marusic I, Chong MS. 2009 Hot-wire spatial resolution issues in wall-bounded turbulence.
Journal of Fluid Mechanics **635**, 103.
10. Marusic I, Mathis R, Hutchins N. 2010 Predictive model for wall-bounded turbulent flow.
Science **329**, 193–196.
11. Mathis R, Hutchins N, Marusic I. 2011 A predictive inner-outer model for streamwise turbulence statistics in wall-bounded flows.
Journal of Fluid Mechanics **681**, 537–566.
12. Jacobi I, McKeon BJ. 2011 Dynamic roughness perturbation of a turbulent boundary layer.
Journal of Fluid Mechanics **688**, 258–296.
13. Jacobi I, McKeon BJ. 2011 New perspectives on the impulsive roughness-perturbation of a turbulent boundary layer.
Journal of Fluid Mechanics **677**, 179–203.
14. Jacobi I, McKeon B. 2013 Phase relationships between large and small scales in the turbulent boundary layer.
Experiments in Fluids **54**, 1–13.
15. Duvvuri S, McKeon BJ. 2015 Triadic scale interactions in a turbulent boundary layer.
Journal of Fluid Mechanics **767**.
16. Chung D, McKeon BJ. 2010 Large-eddy simulation of large-scale structures in long channel flow.
Journal of Fluid Mechanics **661**, 341–364.
17. Ganapathisubramani B, Hutchins N, Monty JP, Chung D, Marusic I. 2012 Amplitude and frequency modulation in wall turbulence.
Journal of Fluid Mechanics **712**, 61–91.
18. Dogan E, Hanson RE, Ganapathisubramani B. 2016 Interactions of large-scale free-stream turbulence with turbulent boundary layers.
Journal of Fluid Mechanics **802**, 79–107.
19. Hearst RJ, Buxton ORH, Ganapathisubramani B, Lavoie P. 2012 Experimental estimation of fluctuating velocity and scalar gradients in turbulence.
Experiments in Fluids **53**, 925–942.
20. Schlatter P, Örlü R. 2010 Quantifying the interaction between large and small scales in wall-bounded turbulent flows: A note of caution.
Physics of Fluids **22**.
21. Mathis R, Marusic I, Hutchins N, Sreenivasan KR. 2011 The relationship between the velocity skewness and the amplitude modulation of the small scale by the large scale in turbulent boundary layers.
Physics of Fluids **23**.
22. Brown GL, Thomas ASW. 1977 Large structure in a turbulent boundary layer.
Physics of Fluids **20**, S243–S252.
23. Robinson SK. 1986 Instantaneous velocity profile measurements in a turbulent boundary layer.
Chemical Engineering Communications **43**, 347–369.
24. Marusic I, Heuer WDC. 2007 Reynolds number invariance of the structure inclination angle in wall turbulence.
Phys. Rev. Lett. **99**, 114504.
25. Mathis R, Marusic I, Hutchins N, Monty J, Harun Z. 2015 Inner-outer interaction predictive model for wall-bounded turbulence subjected to pressure gradient effect.
In *International Symposium on Turbulence and Shear Flow Phenomena (TSFP-9)*.

26. Agostini L, Leschziner MA. 2014 On the influence of outer large-scale structures on near-wall turbulence in channel flow.
Physics of Fluids **26**.
27. Chin CC, Hutchins N, Ooi ASH, Marusic I. 2009 Use of direct numerical simulation (dns) data to investigate spatial resolution issues in measurements of wall-bounded turbulence.
Measurement Science and Technology **20**, 115401–.
28. Guala M, Metzger M, McKeon BJ. 2011 Interactions within the turbulent boundary layer at high reynolds number.
Journal of Fluid Mechanics **666**, 573–604.